Macromolecules

ARTICLE

pubs.acs.org/Macromolecules

Well-Defined Poly(lactic acid)s Containing Poly(ethylene glycol) Side Chains

José A. Castillo,[†] Dorothee E. Borchmann,[†] Amy Y. Cheng,[‡] Yufeng Wang,[†] Chunhua Hu,[†] Andrés J. García,[*,‡] and Marcus Weck[*,†]

[†]Molecular Design Institute and Department of Chemistry, New York University, New York, New York 10003, United States

[‡]Woodruff School of Mechanical Engineering and Institute for Bioengineering and Bioscience, Georgia Institute of Technology, Atlanta, Georgia 30332-0400, United States

Supporting Information

ABSTRACT: Poly(ethylene glycol) (PEG) side-chain functionalized lactide analogues have been synthesized in four steps from commercially available L-lactide. The key step in the synthesis is the 1,3-dipolar cycloaddition between PEG-azides and a highly strained spirolactide−heptene monomer, which proceeds in high conversions. The PEG-grafted lactide analogues were polymerized via ring-opening polymerization using triazabicyclodecene as organocatalyst to give well-defined tri- and hepta(ethylene glycol)−poly(lactide)s (PLA) with molecular weights above 10 kDa and polydispersity indices between 1.6 and 2.1. PEG−poly(lactide) (PLA) with PEG chain M_n 2000 was also prepared, but GPC analysis showed a bimodal profile indicating the presence of starting macromonomer. Cell adhesion assays were performed using MC3T3-E1 osteoblast-like cells demonstrating that PEG-containing PLA reduces cell adhesion significantly when compared to unfunctionalized PLA.

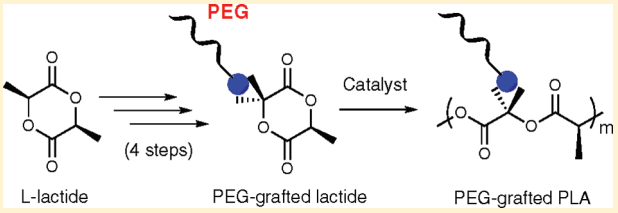

INTRODUCTION

Poly(lactic acid) (PLA), a poly(2-hydroxypropionic acid), is a biodegradable and biocompatible polymer from biorenewable feedstock. Following today's trend of minimizing the impact of chemicals on the environment as well as searching for alternatives to depleting petrochemical resources, PLA is the candidate of choice for polymeric commodities (e.g., packaging materials for food and beverages, plastic bags, and thin film coatings) as well as in the medical field (e.g., for medical devices, sutures, and tissue replacement and as delivery vehicle).[1,2] PLA can be obtained via the polycondensation of lactic acid or the ring-opening polymerization (ROP) of cyclic lactides.[3] One drawback of PLA is its lack of functional side-chain diversity, which limits the possibilities for chemical modification.[2,4] To overcome this limitation, syntheses of modified lactide monomers with functionalized side chains have been reported in the past decade.[2,4−8] We have published the synthesis of cyclic lactides bearing protected alcohols, amines, and carboxylic acid functionalities starting from commercially available amino acids.[9,10] Another versatile synthetic approach has been reported by Yang and co-workers, who have synthesized functional hemilactides through a Passerini-type condensation.[11]

Our ultimate goal is to develop polymeric scaffolds for bone tissue engineering with adequate mechanical properties and controlled architectures that support osteoblast function. Recently, we have reported the synthesis of poly(lactic acid) (PLA)-*block*-poly(norbornene) (PNB) copolymers that bear photo-cross-linkable cinnamate side chains to enhance mechanical strength.[12] In order to improve the properties of these scaffolds further, herein we report the preparation of poly(ethylene glycol) (PEG)-functionalized PLA. We rationalize that this modification should reduce nonspecific protein adsorption, a prerequisite to our scaffold design.[13] It has also been reported that surface PEGylation increases the mechanosensitivity of osteoblasts, i.e., the specific response to mechanical stimulation, and accelerates growth and development of osteoblasts for bone repair and tissue engineering.[14,15]

Several groups have grafted PEG in a random fashion onto PLA. Baker and co-workers reported a postpolymerization modification of propargylglycolide polymers with PEG-azides via Huisgen cycloaddition.[16] Hildgen and co-workers have prepared randomly PEG-grafted PLA to prepare stealth nanoparticles for drug delivery. They initially polymerized D,L-lactide in the presence of allyl glycidyl ether followed by subsequent PEG functionalization.[17] Baker and co-workers have also reported the synthesis of well-defined PEG-grafted PLA based on the condensation of hydroxyacids with PEG side chains. However, this synthetic route consisted of several steps in moderate yields.[18] Despite these elegant approaches, a general approach to prepare well-defined PLA containing PEG side chains still remains a synthetic challenge. In this contribution we report a short and efficient functionalization of L-lactide monomer with PEG side chains and the subsequent

Received: July 17, 2011
Revised: November 14, 2011
Published: December 16, 2011

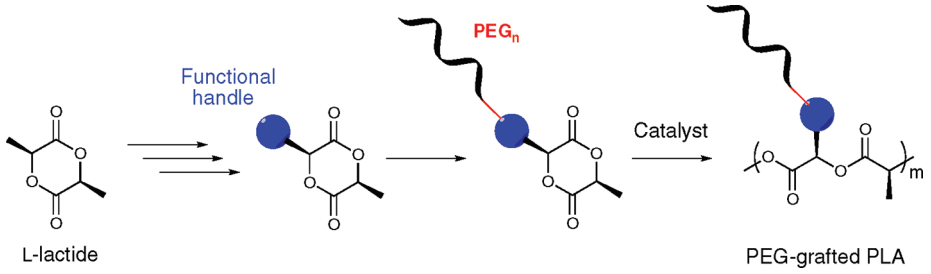

Figure 1. Schematic approach to the preparation of well-defined PEG-grafted PLA from L-lactide.

Scheme 1. General Synthetic Approach To Prepare PEG$_n$-PLA

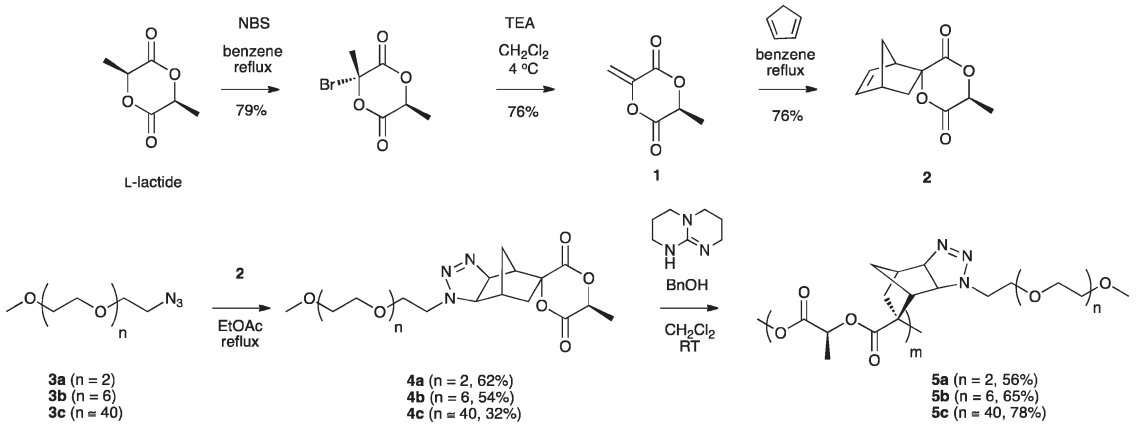

polymerization. Furthermore, since cell adhesion to polymeric surfaces is primarily mediated by adhesive proteins adsorbed from serum such as vitronectin and fibronectin,[19] cell adhesion assays were performed using MC3T3 × 10^{-1} as osteoblast-like cells in order to investigate the reduction of nonspecific protein adsorption caused by the new PEG-grafted polymers.

RESEARCH DESIGN

The main requirement for our research design is that we can functionalize cyclic L-lactide monomers with PEG side chains of different sizes in high yields and in a straightforward fashion in order to prepare well-defined PEG-grafted PLA (Figure 1). Our design is based on some recent work by Jing and Hillmyer, who have reported the synthesis of *exo*-methylene−lactide **1** and spirolactide−heptene **2** (Scheme 1).[20] We rationalized that **2** due to its high ring strain can serve as dipolarophile in cycloaddition reactions. Knowing that azides react readily with strained alkenes such as norbornenes via 1,3-dipolar cycloadditions,[21−23] our hypothesis is that the cycloaddition between PEG-azides and **2** which contains a norbornene moiety might be an easy entranceway toward PEG functionalized cyclic lactides.

EXPERIMENTAL SECTION

Materials. Compounds **1** and **2** were synthesized as described by Jing and Hillmyer.[20] Poly(ethylene glycol) monomethyl ether tosylates **6**, **10**, and **11** were prepared as reported by Ouchi and co-workers.[24] Azido-poly(ethylene glycol) monomethyl ethers **3a**, **3b**, and **3c** were obtained using a methodolgy reported by Saha and Ramakrishnan.[25] Triethylene glycol monomethyl ether (97%), poly(ethylene glycol) methyl ether (M_n ∼ 2000), L-lactide (98%), dicyclopentadiene (97%), 1,5,7-triazabicyclo[4.4.0]dec-5-ene (97%), benzyl alcohol (99.8%), and 1-azidoadamantane (97%) were purchased from Sigma-Aldrich. Tetraethylene glycol (99.5%) was purchased from Acros Organics. Benzene was distilled over sodium and benzophenone under nitrogen before use. Dichloromethane was dried over calcium hydride and distilled under nitrogen prior to use. ^{1}H and ^{13}C NMR spectra were recorded on a Bruker AC 400 spectrometer (400 and 100 MHz for ^{1}H and ^{13}C, respectively). All chemical shifts are reported in parts per million (ppm) with reference to solvent residual peaks. Gel permeation chromatography (GPC) was performed using an HPLC from Agilent Technologies 1200 series and two columns (gel type: AM GPC gel, porosities: 100, 1000, 100 000 Å, linear mixed bed from American Polymer Standards) connected in series with an Optilab rEX refractive index detector from Wyatt Technology. Experiments were performed at room temperature using $CHCl_3$/triethylamine/isopropanol 94:4:2 as eluent, flow rate of 1 mL/min, and molecular weights are reported versus PEG standards (M_n from 1050 to 30 000). Electrospray ionization (ESI) mass spectra were obtained on an Agilent 1100 Series capillary LCMSD trap XCT spectrometer using MeOH/H_2O and ACN/H_2O as eluents. Microwave-assisted reactions were performed using a CEM Discovery microwave reactor. IR spectra were recorded using KBr tablets or poly(ethylene) sample cards on a Nicolet 550 Magna-IR spectrometer. Elemental analysis was performed on a Perkin-Elmer 2400 Series II CHNSO analyzer and by Intertek-QTI. Melting points were determined using a Fisher-Johns apparatus. The MALDI-TOF spectrum of **4c** was recorded on a Bruker UltrafleXtreme using dithranol as matrix and NaCl as doping salt. The sample was prepared following the multiple-layer spotting technique reported by Meier and Schubert.[26] Thermogravimetric analyses were recorded on a Perkin-Elmer Pyris 1TGA from 25 to 550 °C with a heating/cooling rate of 10 °C min^{-1} under N_2. Differential scanning calorimetry (DSC) measurements were acquired

dx.doi.org/10.1021/ma2016387 |*Macromolecules* 2012, 45, 62–69

using a Perkin-Elmer DSC Pyris 1. Samples were run under a nitrogen atmosphere from −10 to 100 °C with a heating/cooling rate of 10 °C min^{-1}. Dialysis membrane Spectra/Por 6, MWCO 1000 and 3500 (38 mm flat width), was purchased from SpectrumLabs and rinsed with water prior to use. About 10 cm of dialysis membrane was used per purification. For **4c** and polymers **5a**−**c**, a dichloromethane solution of product was introduced inside the dialysis bag (MWCO 1000 for macromonomer **4c** and polymers **5a**,**b** and MWCO 3500 for polymer **5c**) that was then introduced to 0.5 L of dichloromethane and gently stirred for about 12 h. Four cycles were performed for each dialysis.

Single Crystal Structure Determination. A colorless block crystal **4d** with the size of 0.12 × 0.22 × 0.30 mm^3 was selected for geometry and intensity data collection with a Bruker SMART APEXII CCD area detector on a D8 goniometer at 100 K. The temperature during the data collection was controlled with an Oxford Cryosystems Series 700 plus instrument. Preliminary lattice parameters and orientation matrices were obtained from three sets of frames. Data were collected using graphite-monochromated and 0.5 mm MonoCap-collimated Mo Kα radiation (λ = 0.710 73 Å) with the ω scan method.[27] Data were processed with the INTEGRATE program of the APEX2 software[27] for reduction and cell refinement. Multiscan absorption corrections were applied by using the SCALE program for area detector. The structure was solved by the direct method and refined on F^2 (SHELXTL).[28] Non-hydrogen atoms were refined with anisotropic displacement parameters, and hydrogen atoms on carbons were placed in idealized positions (C−H = 0.99 or 1.00 Å) and included as riding with U_{iso}(H) = 1.2 or 1.5 U_{eq}(non-H).

Synthesis of Triethylene Glycol Methyl Ether−1,2,3-Δ^2-Triazoline-spiro[6-methyl-1,4-dioxane-2,5-dione-3,2′-bicyclo-[2.2.1]heptane], PEG_3-Spirolactide (4a). Azidotriethylene glycol methyl ether, PEG_3-N_3, **3a** (684 mg, 3.62 mmol), and spiro[6-methyl-1,4-dioxane-2,5-dione-3,2′-bicyclo[2.2.1]hepta-5-ene], **2** (753 mg, 3.62 mmol), were dissolved in EtOAc (20 mL). The reaction was refluxed under nitrogen for 3 days, and the conversion was monitored by ^{1}H NMR spectroscopy. The crude reaction was concentrated under reduced pressure to give a brown oil. This crude product was purified by silica chromatography using EtOAc/hexane 7:3 as eluent to afford the titled triazoline as a yellow oil (897 mg, 62%). ^{1}H NMR ($CDCl_3$, 400 MHz, data shown for major isomer): δ = 5.18 (q, J = 4.9 Hz, 1H, −CH− of LA unit), 4.92 (d, J = 9.8 Hz, 1H, −CH− of triazoline unit), 3.81 (m, 2H), 3.75−3.60 (PEG chain, 12H), 3.57 (m, 3H), 3.37 (s, 3H, CH_3−PEG−), 3.08 (s, 1H), 2.76 (dd, J = 14.3 Hz, J = 5.0 Hz 1H), 2.63 (d, J = 4.9 Hz, 1H), 1.76 (dt, J = 11.7 Hz, J = 1.5 Hz, 1H), 1.69 (d, J = 6.7 Hz, 3H, CH_3− of LA unit), 1.53 (dd, J = 14.1 Hz, J = 3.5 Hz, 1H), 1.28−1.25 (m, 1H). ^{13}C NMR ($CDCl_3$, 100 MHz, data shown for major isomer): δ = 167.9, 167.1, 85.7, 78.7, 73.0, 72.1, 70.8 (×2), 70.7, 70.3, 62.7, 59.2, 49.0, 48.3, 38.3, 31.6, 16.8. ESI-mass: 420.1 (M^++Na^+). MS-ESI $(M + H)^+$ m/z calcd for $C_{18}H_{28}N_3O_7$ 398.42; found 398.1. Elemental analysis: calcd for $C_{18}H_{27}ON_3O_7$: C 54.40, H 6.85, N 10.57; found: C 54.78, H 6.83, N 10.08. IR (KBr) ν (cm^{-1}): 2920.3, 2881.5, 1759.0, 1466.5, 1352.2, 1281.6, 1228.3, 1199.3, 1105.7, 1062.2, 1020.5, 986.9, 851.4, 647.1.

Synthesis of Heptaethylene Glycol Methyl Ether−1,2,3-Δ^2-Triazoline-spiro[6-methyl-1,4-dioxane-2,5-dione-3,2′-bicyclo-[2.2.1]heptane], PEG_7−Spirolactide (4b). Azidoheptaethylen glycol methyl ether, PEG_7-N_3, **3b** (1.30 g, 3.56 mmol), and spiro[6-methyl-1,4-dioxane-2,5-dione-3,2′-bicyclo[2.2.1]hepta-5-ene], **2** (741 mg, 3.56 mmol), were dissolved in EtOAc (20 mL). The reaction was refluxed under nitrogen for 4 days. The conversion after 4 days was measured by ^{1}H NMR spectroscopy to be 78%. The crude reaction was concentrated under reduced pressure to give a brown oil. This solid was purified by silica chromatography using EtOAc/hexane 7:3 as eluent to afford the title triazoline as a yellow oil (1.10 g, 54%). ^{1}H NMR ($CDCl_3$, 400 MHz, data shown for major isomer): δ = 5.18 (q, J = 6.7 Hz, 1H, −CH− of LA unit), 4.90 (d, J = 9.8 Hz, 1H, −CH− of triazoline unit), 3.82 (m, 2H), 3.75−3.61 (PEG chain, 34H), 3.53 (m, 3H), 3.35 (m, 3H, CH_3−PEG−), 3.09 (s, 1H), 2.75 (dd, J = 14.0 Hz, J = 4.9 Hz, 1H), 2.63 (d, J = 4.7 Hz, 1H), 1.78 (m, 1H) (dd, J = 11.6 Hz, J = 1.5 Hz, 1H), 1.69 (d, J = 6.7 Hz, 3H, CH_3− of LA unit), 1.54 (dd, J = 14.1 Hz, J = 3.6 Hz, 1H), 1.26−1.23 (m, 1H). ^{13}C NMR ($CDCl_3$, 100 MHz, data shown for major isomer): δ = 167.9, 167.1, 85.7, 78.7, 73.0, 72.1, 70.8, 70.7 (x2), 70.2, 62.7, 59.2, 48.9, 48.3, 41.0, 38.2. 31.5, 16.7. MS-ESI $(M + H)^+$ m/z calcd for $C_{26}H_{44}N_3O_{11}$ 574.63; found 574.2. Elemental analysis: calcd for $C_{26}H_{43}N_3O_{11}$: C 54.44, H 7.56, N 7.33; found: C 54.85, H 7.76, N 7.12. IR (KBr) ν (cm^{-1}): 2922.3, 2870.3, 2105.6, 1957.5, 1757.7, 1466.3, 1350.9, 1282.0, 1140.8, 1062.6, 986.7, 937.0, 851.7, 743.7, 685.7, 649.0, 571.1.

Synthesis of Poly(ethylene glycol methyl ether)−1,2,3-Δ^2-Triazoline-spiro[6-methyl-1,4-dioxane-2,5-dione-3,2′-bicyclo-[2.2.1]heptane] (M_n ∼ 2200), PEG_{40}−Spirolactide (4c). Azido-poly(ethylene glycol methyl ether) (M_w∼ 2000), PEG_{40}-N_3, **3c** (3.35 g, 1.67 mmol), and spiro[6-methyl-1,4-dioxane-2,5-dione-3,2′-bicyclo[2.2.1]hepta-5-ene], **2** (1.26 mg, 6.0 mmol, 3.6 equiv), were dissolved in EtOAc (40 mL). The reaction was refluxed under nitrogen for 3 days. The crude reaction was concentrated under reduced pressure to afford a dark green solid. The crude product was dissolved in CH_2Cl_2 (∼15 mL), and diethyl ether was added (∼30 mL). The suspension was refluxed for 20 min and cooled down to room temperature, affording a white suspension and a green oil. The layers were separated, and the white suspension was cooled down to 4 °C when a white solid precipitated. This solid was washed with diethyl ether. The crystallyzation was repeated two more times, affording the title compound as a white solid (1.17 g, 32%). The monomer was dialyzed in CH_2Cl_2 using a cellulose membrane (MWCO 1000). Finally, compound **4c** was lyophilized twice from distilled benzene (3 times distilled) prior to polymerization. ^{1}H NMR ($CDCl_3$, 400 MHz, data shown for major isomer): δ = 5.17 (q, J = 6.6 Hz, 1H, −CH− of LA unit), 4.92 (d, J = 9.7 Hz, 1H, −CH− of triazoline unit), 3.73−3.45 (PEG chain), 3.45 (m, 3H), 3.36 (m, 3H, CH_3−PEG−), 3.08 (s, 1H), 2.75 (dd, J = 14.0 Hz, J = 4.9 Hz, 1H), 2.62 (d, J = 4.6 Hz, 1H), 1.87 (dd, J = 11.6 Hz, J = 1.3 Hz, 1H), 1.68 (d, J = 6.7 Hz, 3H, CH_3− of LA unit), 1.53 (dd, J = 14.1 Hz, J = 3.7 Hz, 1H), 1.24 (m, 1H). ^{13}C NMR ($CDCl_3$, 100 MHz, data shown for major isomer): δ = 167.9, 167.0, 88.6, 85.7, 78.7, 77.4, 70.3 (PEG chain), 62.7, 59.2, 56,1, 49.0, 48.3, 44.9, 41.0, 40.0, 39.5, 38.3, 31.6, 27.3, 16.8. Melting point: 45−46 °C. Elemental analysis: calcd for $C_{94}H_{218}N_3O_{45}$: C 53.55, H 10.3, N 2.0; found: C 53.79, H 8.61, N 1.08. IR (KBr) ν (cm^{-1}): 2921.3, 2882.4, 2242.3, 2098.6, 2058.5, 1954.3, 1758.6, 1467.0, 1343.2, 1280.6, 1241.9, 1112.8, 963.0, 843.0, 742.8, 569.8.

Synthesis of Adamantyl-1,2,3-Δ^2-triazoline−Spiro[6-methyl-1,4-dioxane-2,5-dione-3,2′-bicyclo[2.2.1]heptane] (4d). 1-Azidoadamantante (255 mg, 1.44 mmol) and spiro[6-methyl-1,4-dioxane-2,5-dione-3,2′-bicyclo[2.2.1]hepta-5-ene], **2** (300 mg, 1.44 mmol), were dissolved in EtOAc. The reaction was refluxed overnight under nitrogen. The crude reaction was concentrated under reduced pressure to afford an orange solid. The crude product was purified by silica chromatography using EtOAc/hexane 8:2 as eluent to afford the title triazoline as a white solid (290 mg, 52%). ^{1}H NMR ($CDCl_3$, 400 MHz, data shown for major isomer): δ = 5.22 (q, J = 6.7 Hz, 1H, −CH− of LA unit), 4.84 (d, J = 9.9 Hz, 1H, −CH− of triazoline unit), 3.65 (d, J = 9.9 Hz, 1H, −CH′− of triazoline unit), 3.13 (s, 1H), 2.73 (dd, J = 14.1 Hz, J = 4.9 Hz, 1H), 2.42 (d, J = 5.2 Hz, 1H), 2.15−2.08 (m, 7H), 1.86−1.79 (m, 4H), 1.78−1.66 (m, 10H, CH_3− of LA unit and adamantane unit), 1.56 (dd, J = 14.1 Hz, J = 4.6 Hz, 1H), 1.30−1.27 (m, 1H). ^{13}C NMR ($CDCl_3$, 100 MHz, data shown for major isomer): δ = 168.0, 167.2, 86.1, 78.2, 73.0, 58.4, 57.4, 49.1, 43.8, 42.2, 36.4, 31.7, 29.6, 16.8. Melting point: 214−215 °C. MS-ESI $(M + H)^+$ m/z calcd for $C_{21}H_{28}N_3O_4$ 386.46; found 386.2. Elemental analysis: calcd for $C_{21}H_{27}N_3O_4$: C 65.44, H 7.06, N 10.9; found: C 65.53, H 7.00, N 10.9. IR (KBr) ν (cm^{-1}): 3533.7, 3497.0, 2997.3, 2917.6, 2851.5, 2680.6, 2333.5, 1750.1, 1482.3, 1454.8, 1360.3, 1313.2, 1242.6, 1147.6, 1086.6, 1020.0, 987.4, 928.6, 855.7, 826.2, 787.1, 737.5, 693.1, 647.5, 582.3, 485.7.

Scheme 2. 1,3-Dipolar Cycloaddition between 1-Azidoadamantane and Spirolactide 2

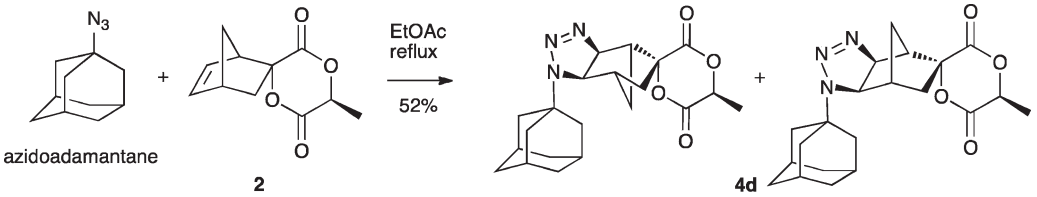

General Procedure for Microwave-Assisted 1,3-Dipolar Cycloaddition. PEG_n-azide (1 equiv) and spirolactide (1 equiv) were mixed in a tube reactor in the absence of solvent. The reaction mixture was irradiated using microwave irradiation at 70 °C for 3 cycles (each 1 h) at 150 W. The conversion was followed by ^1H NMR spectroscopy.

Polymerization. All L-lactide analogues were stored under nitrogen in a freezer to ensure stability. Prior to polymerization, monomers **4a,b** were triply recrystallized from EtOAc/hexane while monomer **4c** was triply recrystallized from CH_2Cl_2/diethyl ether. Then, each monomer was frozen in benzene (triply distilled) and lyophilized (3×). The polymerization of **4a** is described as an example. In a nitrogen-filled glovebox, a catalyst/initiator solution was prepared by combining 1,5,7-triazabicyclo-[4.4.0]dec-5-ene (TBD, 18 mg, 0.126 mmol), benzyl alcohol (26 μL, 0.251 mmol), and anhydrous CH_2Cl_2 (25 mL) in a 25 mL volumetric flask. The freshly prepared catalyst/initiator solution (730 μL) was added to the Schlenk flask containing **4a** (290 mg, 0.73 mmol). The initial concentrations were **4a** 1 M (100 equiv), TBD 0.5 equiv, and BnOH 1 equiv. After 24 h, the crude reaction was concentrated under reduced pressure and purified by dialysis (MWCO 1000) from CH_2Cl_2. Polymer **5a** was isolated as a yellow oil (255 mg, 56%). ^1H NMR (acetone-d_6, 400 MHz): δ = 5.34−4.70 (m, 2H, −CH- of LA unit and −CH− of triazoline unit), 3.81 (m, 1H), 3.71 (m, 3H), 3.60 (PEG chain, 8H), 3.48 (m, 2H), 3.30 (s, 3H, CH_3−PEG−), 3.23−2.78 (m, 2H), 2.62−2.47 (m, 2H), 1.75 (m, 1H), 1.56 (m, 4H, including CH_3− of LA unit), 1.36 (m, 1H). 1.09 (m, 1H). ^{13}C NMR (acetone-d_6, 100 MHz): δ = 170.8, 170.6, 85.0, 80.7, 72.7, 71.1, 70.5, 63.0, 59.0, 50.0, 48.9, 42.4, 37.8, 29.9, 17.1. Elemental analysis: calcd for $C_{18}H_{27}N_3O_7$: C 54.40, H 6.85, N 10.57; found: C 55.12, H 7.27, N 9.65.

PEG_7-Grafted PLA (5b). Polymer **5b** was prepared as described above and isolated as a yellow oil (454 mg, 65%). ^1H NMR (acetone-d_6, 400 MHz): δ = 5.35−4.55 (m, 2H, −CH− of LA unit and −CH− of triazoline unit), 3.85 (m, 1H), 3.72 (m, 4H), 3.59 (PEG chain, 30H), 3.48 (m, 3H), 3.30 (s, 4H, including CH_3−PEG−), 3.24−2.95 (m, 1H), 2.75−2.54 (m, 2H), 1.75 (m, 1H), 1.59 (m, 5H, including CH_3− of LA unit), 1.36 (m, 1H). 1.11 (m, 1H). ^{13}C NMR (acetone-d_6, 100 MHz): δ = 170.9, 170.7, 85.2, 80.6, 70.6, 63.0, 55.1, 48.9, 42.4, 41.9, 29.9, 17.0. Elemental analysis: calcd for $C_{26}H_{43}N_3O_{11}$: C 54.44, H 7.56, N 7.33; found: C 53.57, H 7.72, N 6.90.

PEG_{40}-Grafted PLA (5c). Polymer **5c** was prepared as described above; in this case the initial concentration of monomer **4c** was 0.33 M (100 equiv), TBD 1.5 equiv, and BnOH 3.0 equiv. Polymer **5c** was purified by dialysis (MWCO 3500) from CH_2Cl_2, resulting in a white solid (454 mg, 78%). Melting point: 45−46 °C. ^1H NMR (acetone-d_6, 400 MHz): δ = 5.27 (m, 1H, −CH− of LA unit), 3.91−3.51 (PEG chain, 349H), 3.46 (m, 5H), 3.29 (s, 6H, including CH_3−PEG−), 3.10 (m, 2H), 2.81 (m, 11H), 2.63 (m, 2H), 2.50 (m, 1H), 1.65−1.47 (m, 5H, including CH_3− of LA unit), 1.41 (m, 1H), 1.29 (m, 1H). 1.08 (m, 1H). ^{13}C NMR (acetone-d_6, 100 MHz): δ = 162.1, 170.7, 94.8, 86.5, 77.7, 71.4, 69.6, 63.7, 60.6, 58.9, 49.9, 49.0, 39.0, 29.5, 16.7. Elemental analysis: calcd for $C_{94}H_{218}N_3O_{45}$: C 53.55, H 10.3, N 2.0; found: C 54.08, H 9.01, N 1.11.

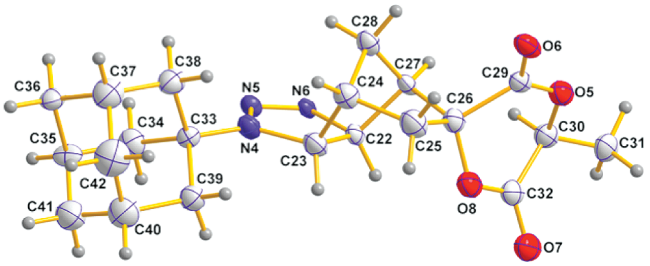

Figure 2. Crystal structure of one isomer of azidomantane−spirolactide **4d**.

Cell Adhesion Assay. Glass slides were spin-coated with polymer solutions (100 mg/5 mL $CHCl_3$) at 500 rpm for 10 s and then at 3000 rpm for 30 s. After air drying, the slides were rinsed with deionized water, 70% ethanol, and Dulbecco's phosphate-buffered saline (DPBS, Invitrogen). MC3T3-E1 osteoblast-like cells (RIKEN Cell Bank) at passage 12 were seeded on coated slides at a cell density of 10 000 cells/cm^2 in serum-containing media (α-MEM supplemented with 10% fetal bovine serum). At 4 h, cells were permeabilized for 3 min in DPBS containing 0.5% Triton X-100 and fixed in 4% paraformaldehyde for 10 min. Slides were blocked in complete DPBS containing 5% goat serum and 0.01% NaN_3 for 1 h and subsequently incubated with antivinculin antibodies (1:400, Upstate Biotechnology V284) and 4′,6-diamidino-2-phenylindole (DAPI, Sigma) in blocking buffer for 1 h. AlexaFluor488-conjugated secondary antibody (Invitrogen) was then incubated for 1 h. Slides were mounted with antifade reagent and viewed with a Nikon E400 fluorescence microscope using 10× and 40× objectives. Images were acquired with SPOT Advanced Software (Diagnostic Instruments, Inc.). To quantify cell adhesion, fluorescence images were analyzed with the ImageJ software (v1.44, NIH) to determine average cell numbers. Cell counts were analyzed using ANOVA with Tukey's test for pairwise comparisons.

RESULTS AND DISCUSSION

Our synthetic strategy to functionalize L-lactide with PEG side chains started with the preparation of spirolactide−heptene **2** according to literature procedures, which was prepared as a mixture of diastereomers (Scheme 1).[20]

We investigated initially whether **2** can react as a dipolarophile in 1,3-dipolar cycloadditions. Since the 1,3-dipolar cycloaddition between 1-azidoadamantane and norbornene has been reported in the literature,[23] we studied, as a proof of concept, the 1,3-dipolar cycloaddition between 1-azidoadamantane and **2** (Scheme 2). The reaction was carried out in EtOAc at reflux. Within 12 h, high conversions of the 1,2,3-Δ^2-triazoline isomers were obtained as characterized by TLC analyses. ^1H NMR spectroscopy analysis showed the disappearance of the alkene signals of **2** as well as the formation of two new doublets at 4.84 and 3.65 ppm, which is in good agreement with the chemical shifts of the Δ'-1,2,3-triazoline

dx.doi.org/10.1021/ma2016387 |*Macromolecules* 2012, 45, 62–69

Table 1. Polymer Characterization Data

polymer	M_n $(10^{-3})^a$	PDI[a]	t_R (min)[a]	X_n[b]	M_n $(10^{-3})^c$	conv[d] (%)	yield[e] (%)
PEG_3-PLA **5a**	12	2.1	18.3	30	44	99	60
PEG_7-PLA **5b**	14	1.6	18.3	24	270	82	54
PEG_{40}-PLA **5c**	11	1.4	18.3	5	3200	50	78[f]

[a] GPC in $CHCl_3$/TEA/isopropanol 94:4:2 with PEG standards using refractive index for detection. [b] Degree of polymerization (X_n) calculated from GPC analyses. [c] Number-average molecular weight determined based on ^{1}H NMR end-group analysis. [d] Conversion of polymerization measured by ^{1}H NMR spectroscopy. [e] Isolated yield of polymerization after purification by dialysis in CH_2Cl_2. [f] Polymer **5c** was contaminated with starting macromomoner **4c**.

ring protons reported for the corresponding norbornene adduct with azidoadamantane.[23] The crude reaction was purified by silica gel column chromatography and recrystallized from EtOAc/hexane, affording a mixture of two isomers in a ratio of 1.0:0.4. Single crystal X-ray analysis confirmed the formation of two isomers of **4d** (Scheme 2, Figure 2, and Supporting Information).

After our model reaction afforded the desired cycloaddition product, we investigated the functionalization of **2** with poly(ethylene glycol) moieties. With this aim, we synthesized the three PEG-azides **3a** and **3c** via tosylation and azidation of the corresponding commercially available poly(ethylene glycol) methyl ether using standard conditions (i.e., p-TsCl and NaOH in H_2O/THF and NaN_3/DMF, respectively).[25] In the case of PEG-azide **3b**, we previously synthesized the starting heptaethylene glycol methyl ether (see Scheme S1 in the Supporting Information). The 1,3-dipolar cycloaddition between PEG_3-N_3 **3a** and **2** carried out in EtOAc under reflux for 12 h gave the desired PEG_3-spirolactide **4a**. ^{1}H NMR spectroscopy analyses showed the formation of a new doublet at 4.91 ppm, corresponding to one of the two Δ′-1,2,3-triazoline ring protons, with similar chemical shift and coupling constants to those reported above for the triazoline **4d**. The second doublet overlapped with the PEG chain signal in the ^{1}H NMR spectrum. However, it could be observed easily at 3.65 ppm in the COSY NMR spectrum (Supporting Information). The doublet at 4.91 ppm served as criterion for us to monitor the progress of the reaction by NMR spectroscopy. After 3 days at reflux, the observed conversion was 94%. Based on ^{1}H NMR spectroscopy analyses of the crude reaction mixture, two triazoline isomers were obtained in a ratio of 1.0:0.45. In addition, ^{13}C NMR spectroscopy analysis showed two signals at 168.0 and 167.1 ppm corresponding to the two carbonyl groups on the lactide ring, indicating that the ring was conserved during the cycloaddition and the purification process. The IR spectrum of **4a** does not show a signal corresponding to the starting azide, and the ESI mass spectrum of **4a** showed one signal at 398.1 m/z $(M + H)^+$.

After preparing **4a** successfully (62% yield after silica chromatography), we applied our methodology to azides **3b**, PEG_7-N_3, and **3c**, PEG_{40}-N_3, $M_w \sim 2000$. The 1,3-dipolar cycloadditions between PEG_7-N_3 **3b** and PEG_{40}-N_3 **3c** with **2** in EtOAc at reflux for 3−4 days afforded PEG_7-spirolactide **4b** and PEG_{40}-spirolactide **4c**, respectively, in high conversions (75−80% by ^{1}H NMR spectroscopy). Monomer **4b** was purified by silica chromatography (54% isolated yield), and monomer **4c** was triply recrystallized from a 1:5 mixture of CH_2Cl_2/diethyl ether (32% isolated yield). The MALDI-TOF spectrum for **4c** showed masses from 1713 to 2595 (theoretical $M_n \sim 2200$) (Supporting Information). The 1,3-dipolar cycloaddition was also investigated using microwave irradiation to explore whether microwave irradiation can result in shorter reaction times. The microwave-assisted cycloaddition between **3a** and **2** in an equimolar ratio reached a maximum of 86% conversion after 3 h at 70 °C as observed by ^{1}H NMR spectroscopy. In the case of the cycloaddition between **3c** and **2** in equimolar ratio, the conversion observed was 68% after 3 h at 70 °C. When using the spirolactide **2** in slight excess (**3c**:**2** ratio of 1:1.5 equiv), the reaction proceeded to full conversion.

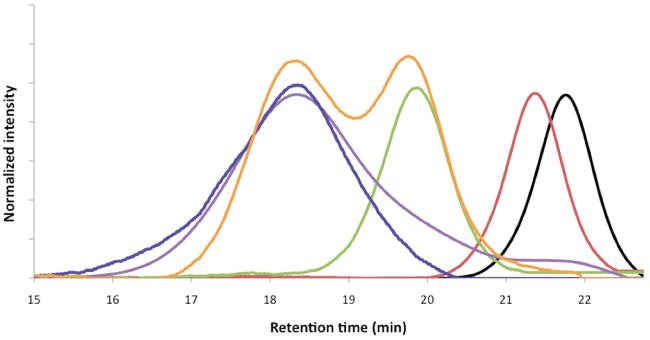

Figure 3. GPC curves of all monomers and polymers in $CHCl_3$/TEA/isopropanol 94:4:2. GPC trace of **4a** (black trace), **4b** (red trace), **4c** (green trace), **5a** (purple trace), **5b** (blue trace), and **5c** (orange trace). All molecular weights are reported versus PEG standards using refractive index for detection.

After the successful synthesis of our three target monomers, we investigated the ring-opening polymerization of **4a**−**c**. The monomers were obtained as a mixture of diastereomers, and we assume that they might possess slightly different reactivities. It is well-known that the ROP of lactides requires high monomer purity,[9,20] and each monomer was purified and dried extensively as can be seen from the Experimental Section. Initially, we investigated the ROP of **4a** using the polymerization conditions reported by us: $SnOct_2$ as catalyst and benzyl alcohol as initiator without solvent under N_2 at 140 °C overnight.[9] Unfortunately, **4a** was not stable under these reactions conditions. Next, we investigated the conditions employed by Hillmyer and co-workers to polymerize **2** (100 equiv) using triazabicyclodecene (TBD, 0.5 equiv) as organocatalyst and benzyl alcohol (1 equiv) as co-initiator.[20] This methodology ensures the preparation of PLA without any metal impurities, which is crucial for the use of our materials in regenerative medicine.[29] The polymerization of **4a** at room temperature after 24 h using the Hillmyer procedure was almost quantitative as measured by ^{1}H NMR spectroscopy. We hypothesize that BnOH attacks the less sterically hindered carbonyl group of the lactide ring, i.e., the carbonyl next to the methyl group.

The kinetics of the polymerization of **4b** was investigated by ^{1}H NMR spectroscopy, showing a maximum of 82% conversion

dx.doi.org/10.1021/ma2016387 |*Macromolecules* 2012, 45, 62–69

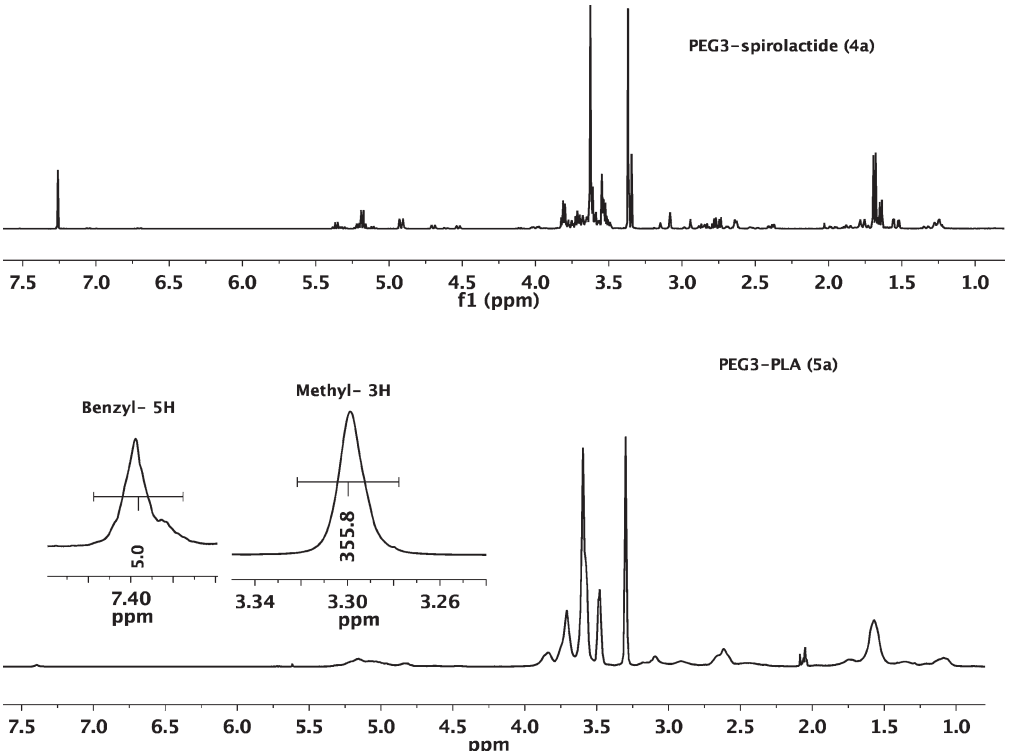

Figure 4. ^{1}H NMR spectrum of PEG$_3$-spirolactide **4a** in $CDCl_3$ (top) and end-group analysis of PEG$_3$-PLA **5a** by the ^{1}H NMR spectrum in acetone-d_6 (bottom).

after 20 h. In the case of monomer **4c**, which is a solid at room temperature and contains a long PEG chain ($M_n \sim 2200$), we decided to dilute the reaction mixture to increase the solubility of the monomer as well as the concentration of the catalyst and co-initiator. The initial concentrations used were **4c** 0.33 M (100 equiv), TBD 1.5 equiv, and BnOH 3 equiv. The polymerization of **4c** was followed by ^{1}H NMR spectroscopy, showing a maximum conversion (~50%) after 36 h. The spectrum of the crude reaction showed two similar and overlapping singlets at 3.29 and 3.30 ppm corresponding to the terminal methyl group of the CH_3-PEG chain (Supporting Information). These two singlets suggest that **4c** and **5c** were present in the crude reaction in similar ratios. We hypothesize that the long PEG chain hinders the polymerization process. Since **4c** is a macromonomer, the long PEG side chain could adopt a random coil conformation that could "internalize" the lactide unit. This conformation would limit catalyst accessibility and thus significantly impede polymerization. Furthermore, the long PEG side chains of the monomers might entangle with the polymer PEG side chains, limiting monomer diffusion.

Isolated yields of all polymers ranged from 54 to 78% (Table 1) after extensive purification by dialysis in CH_2Cl_2 and lyophilization. All polymers were characterized by ^{1}H NMR and ^{13}C NMR spectroscopies, gel-permeation chromatography (GPC), and thermogravimetric analysis (TGA) (Table 1 and Supporting Information). In case of polymer **5c**, after purification by dialysis (MWCO 3500), the ^{1}H NMR spectrum showed again both singlets at 3.3 ppm in similar ratio, indicating that the dialysis process was unsuccessful in removing **4c**.

GPC analyses of the polymers show number-average molecular weights between 11 and 14 kDa and PDI values between 1.4 and 2.1. All values are reported versus PEG standards. We cannot exclude trace contamination of monomers with water due to the hydrophilic PEG side chains despite careful repurifications and lyophilizations using distilled benzene as solvent. The presence of these water molecules might compete with BnOH as co-initiator and would explain the higher than expected PDI values. As expected, GPC analyses of polymers **5a**−**c** show lower retention times (t_R 18.3 min for all three polymers) than monomers **4a**−**c** (Figure 3). The GPC chromatogram of PEG$_{40}$-PLA 5c shows a bimodal profile with a second peak at 19.7 min. This peak overlaps with the signal of the monomer **4c**. Therefore, in the case of polymer **5c**, the PDI value 1.4 was measured in the region of the GPC curve centered at 18 min. That result is in agreement with the NMR spectroscopy data, suggesting that polymer **5c** was still contaminated with the macromonomer **4c** (M_n 2200) after dialysis using a membrane bag MWCO 3500.

Molecular weights of **5a**−**c** were also determined by ^{1}H NMR end-group analysis comparing the integration of the methyl ether group (CH_3-PEG chain) to the benzyl group of the co-initiator (Figure 4). The disagreement between the molecular weights determined by ^{1}H NMR end-group analysis (44 kDa for **5a**, 270 kDa for **5b**, and 3200 kDa for **5c**) and GPC might be due to the high error measuring the small signal in the ^{1}H NMR spectrum corresponding to the co-initiator (benzyl group). Besides, the average molecular weights measured by GPC are not accurate since linear PEG standards were used for calibration while the PEG-grafted polymers **5a**−**c** are brush polymers. The PEG-grafted PLAs have smaller hydrodynamic volumes than linear PEG standards, and consequently, the apparent molecular weight measured by GPC are smaller than that estimated by ^{1}H NMR spectroscopy. Hillmyer and co-workers have recently reported that the polymerization of aliphatic spirolactide derivatives affords polyesters with higher glass transition temperatures than

dx.doi.org/10.1021/ma2016387 |*Macromolecules* 2012, 45, 62–69

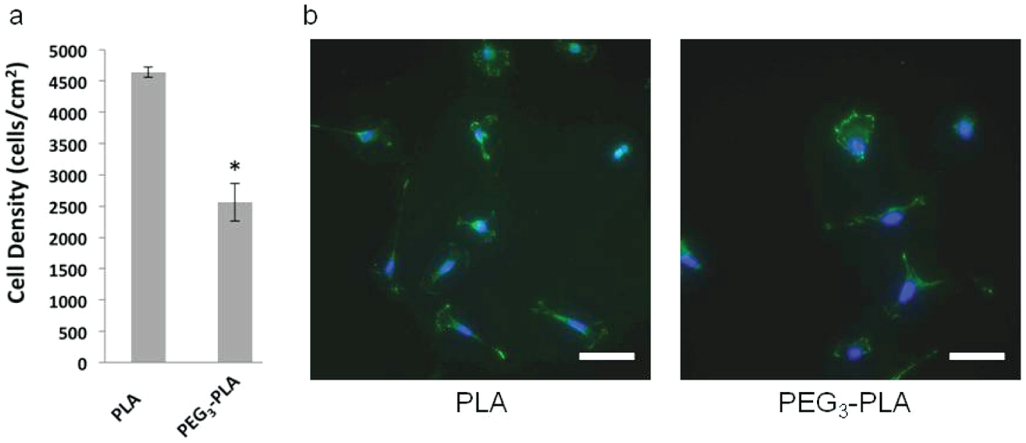

Figure 5. MC3T3-E1 cell adhesion and spreading on spin-coated polymer films. (a) Average density of adherent cells on polymer coatings. Error bars represent standard error of the mean. *P < 0.01compared to PLA. (b) Representative images of adherent cells on polymer films with stained nuclei (DAPI, blue) and focal adhesion protein vinculin (vinc, green). Scale bars are 50 μm.

PLA ($T_g \sim 50$ °C).[30] In contrast, differential scanning calorimetry (DSC) measurements of PEG_3-PLA **5a** and PEG_7-PLA **5b**, which are oils at room temperature, did not show any transition between −10 and 100 °C (Supporting Information). PEG_{40}-PLA **5c** showed a sharp transition around 50 °C, which corresponds to its melting point. Thermogravimetric analysis (TGA) was used to evaluate the thermal stability of polymers **5a**−**c** (Supporting Information). The degradation of **5a** starts at 215 °C, **5b** at 285 °C, and **5c** at 332 °C. Hence, the length of the PEG side chain slightly increases the thermal stability of PEG-grafted polymers.

Cell adhesion studies were performed in order to investigate the capability of the new PEG-grafted PLAs to reduce nonspecific protein adsorption and cell adhesion. Hence, MC3T3 × 10^{-1} cells were seeded in the presence of serum-containing media on PLA (control) and PEG_3-PLA films to examine initial cell adhesion responses. We only examined adhesion to the shorter PEG_3-PLA polymer because the longer PEG chain polymers (PEG_7-PLA and PEG_{40}-PLA) exhibited high water solubility and were rapidly lost from the surface in aqueous solutions. We note that the increased water solubility of the longer PEG chain polymers will be advantageous in future studies dealing with cross-linked scaffolds. The osteoblast-like cells adhered and spread on both PLA and PEG_3-PLA films, but clear differences between PEG-functionalized and control PLA can be seen in cell density and cell morphology. Figure 5a shows that the number of adhered cells was significantly decreased for the PEG-functionalized PLA compared to PLA. Although cells assembled vinculin-containing focal adhesions on both polymer films, differences in morphology were evident (Figure 5b). Cells on PLA were more spread and polarized with focal adhesions localized to the cell tips, whereas cells on PEG_3-PLA showed less spread cells. The differences in cell adhesion and spreading are likely due to differences in protein adsorption between the polymeric films due to the protein adsorption-resistant nature of PEG. The cell adhesion results demonstrate that the addition of PEG chains to PLA modulates biological responses to the base PLA. These results are consistent with previous reports demonstrating changes in cell adhesion following grafting of PEG. Future studies will examine cellular responses within PEG-functionalized PLA scaffolds.

CONCLUSIONS

In this contribution, we have presented a short and general approach to prepare PEG side-chain functionalized L-lactide monomers and their subsequent polymerization. The PEG-spirolactide-based monomers were prepared readily in four steps from commercially available L-lactide in good yields. The key step is the 1,3-dipolar cycloaddition between PEG-azides and the spirolactide−heptene precursor. The monomers were polymerized using TBD as organocatalyst yielding well-defined oligo(ethylene glycol)-functionalized poly(lactic acid) with molecular weights above 10 kDa and polydispersity indices between 1.6 and 2.1. In the case of PEG_{40}-PLA, the measured PDI was 1.4, but the GPC analysis showed a bimodal profile indicating the presence of starting macromonomer despite purification by dialysis. Preliminary biological studies showed that PEG_3-grafted PLA reduces cell adhesion when compared to PLA.

ASSOCIATED CONTENT

Supporting Information. Detailed spectroscopic data and crystallographic data. This material is available free of charge via the Internet at http://pubs.acs.org.

AUTHOR INFORMATION

Corresponding Author

*E-mail: marcus.weck@nyu.edu (M.W.); andres.garcia@me.gatech.edu (A.J.G.).

ACKNOWLEDGMENT

Financial support has been provided by the National Institute of Health (5R01EB008069). The MALDI instrument was purchased with a grant from the National Science Foundation (CHE-0958457).

REFERENCES

(1) Auras, R.; Lim, L.-T.; Selke, S. E. M.; Tsuji, H. *Poly(Lactic Acid): Synthesis, Structures, Properties, Processing, and Applications*; John Wiley & Sons, Inc.: Hoboken, NJ, 2010.

(2) Becker, J. M.; Pounder, R. J.; Dove, A. P. *Macromol. Rapid Commun.* **2010**, *31*, 1923–1937.

(3) Platel, R. H.; Hodgson, L. M.; Williams, C. K. *Polym. Rev.* **2008**, *48*, 11–63.
(4) Pounder, R. J.; Dove, A. P. *Polym. Chem.* **2010**, *1*, 260–271.
(5) Edlund, U.; Kallrot, M.; Albertsson, A.-C. *J. Am. Chem. Soc.* **2005**, *127*, 8865–8871.
(6) Vogeley, N. J.; Baker, G. L.; Smith, M. R., III *Polym. Prepr. (Am. Chem. Soc., Div. Polym. Chem.)* **2005**, *46*, 336.
(7) Leemhuis, M.; van Nostrum, C. F.; Kruijtzer, J. A. W.; Zhong, Z. Y.; ten Breteler, M. R.; Dijkstra, P. J.; Feijen, J.; Hennink, W. E. *Macromolecules* **2006**, *39*, 3500–3508.
(8) Cohen-Arazi, N.; Katzhendler, J.; Kolitz, M.; Domb, A. J. *Macromolecules* **2008**, *41*, 7259–7263.
(9) Gerhardt, W. W.; Noga, D. E.; Hardcastle, K. I.; García, A. J.; Collard, D. M.; Weck, M. *Biomacromolecules* **2006**, *7*, 1735–1742.
(10) Noga, D. E.; Petrie, T. A.; Kumar, A.; Weck, M.; García, A. J.; Collard, D. M. *Biomacromolecules* **2008**, *9*, 2056–2062.
(11) Rubinshtein, M.; James, C. R.; Young, J. L.; Ma, Y. J.; Kobayashi, Y.; Gianneschi, N. C.; Yang, J. *Org. Lett.* **2010**, *12*, 3560–3563.
(12) Wang, Y.; Noga, D. E.; Yoon, K.; Wojtowicz, A. M.; Lin, A. S. P.; García, A. J.; Collard, D. M.; Weck, M. *Adv. Funct. Mater.* **2008**, *18*, 3638–3644.
(13) Heuberger, M.; Drobek, T.; Spencer, N. D. *Biophys. J.* **2005**, *88*, 495–504.
(14) Subramani, K.; Birch, M. A. *Biomed. Mater.* **2006**, *1*, 144–154.
(15) Hamamura, K.; Weng, Y.; Zhao, J.; Yokota, H.; Xie, D. *Biomed. Mater.* **2008**, *3*, 025017–025023.
(16) Jiang, X.; Vogel, E. B.; Smith, M. R.; Baker, G. L. *Macromolecules* **2008**, *41*, 1937–1944.
(17) Sant, S.; Nadeau, V.; Hildgen, P. *J. Controlled Release* **2005**, *107*, 203–214.
(18) Jiang, X.; Milton, R.; Smith; Baker, G. L. *Macromolecules* **2008**, *41*, 318–324.
(19) García, A. J. *Biomaterials* **2005**, *26*, 7525–7529.
(20) Jing, F.; Hillmyer, M. A. *J. Am. Chem. Soc.* **2008**, *130*, 13826–13827.
(21) Dahl, R. S.; Finney, N. S. *J. Am. Chem. Soc.* **2004**, *126*, 8356–8357.
(22) Bräese, S.; Friedrich, A.; Gartner, M.; Schröeder, T. *Top. Heterocycl. Chem.* **2008**, *12*, 45–115.
(23) Sasaki, T.; Eguchi, S.; Yamaguchi, M.; Esaki, T. *J. Org. Chem.* **1981**, *46*, 1800–1804.
(24) Ouchi, M.; Inoue, Y.; Liu, Y.; Nagamune, S.; Nakamura, S.; Wada, K.; Hakushi, T. *Bull. Chem. Soc. Jpn.* **1990**, *63*, 1260–1262.
(25) Saha, A.; Ramakrishnan, S. *Macromolecules* **2009**, *42*, 4956–4959.
(26) Meier, M. A. R.; Schubert, U. S. *Rapid Commun. Mass Spectrom.* **2003**, *17*, 713–716.
(27) APEX2 *(version 2009.11-0). Program for Bruker CCD X-ray Diffractometer Control*; Bruker AXS Inc.: Madison, WI, 2009.
(28) Sheldrick, G. M. *SHELXTL, version 6.14. Program for solution and refinement of crystal structures*; Universität Göttingen: Göttingen, Germany, 2000.
(29) Pratt, R. C.; Lohmeijer, B. G. G.; Long, D. A.; Waymouth, R. M.; Hedrick, J. L. *J. Am. Chem. Soc.* **2006**, *128*, 4556–4557.
(30) Fiore, G. L.; Jing, F.; Young, J. V. G.; Cramer, C. J.; Hillmyer, M. A. *Polym. Chem.* **2010**, *1*, 870–877.
(31) Göpferich, A.; Peter, S. J.; Lucke, A.; Lu, L.; Mikos, A. G. *J. Biomed. Mater. Res.* **1999**, *46*, 390–398.
(32) Iguerb, O.; Poleunis, C.; Mazeas, F.; Compere, C.; Bertrand, P. *Langmuir* **2008**, *24*, 12272–12281.